Future projections of wind energy potentials in the Arctic for the 21st century under the RCP8.5 scenario from regional climate models (Arctic-CORDEX)

Mirseid Akperov[1], Alexey V. Eliseev[1,3,18], Annette Rinke[2], Igor I. Mokhov[1,3], Vladimir A. Semenov[1,4], Mariya Dembitskaya[1], Heidrun Matthes[2], Muralidhar Adakudlu[19], Fredrik Boberg[15], Jens H. Christensen[5,6,14], Klaus Dethloff[2], Xavier Fettweis[7], Oliver Gutjahr[8,9], Günther Heinemann[10], Torben Koenigk[11,12], Dmitry Sein[13], René Laprise[14], Ruth Mottram[15], Oumarou Nikiéma[14], Stefan Sobolowski[5], Katja Winger[14], and Wenxin Zhang[16,17]

[1]A.M. Obukhov Institute of Atmospheric Physics, RAS, Moscow, Russia

[2]Alfred Wegener Institute, Helmholtz Centre for Polar and Marine Research, AWI, Potsdam, Germany

[3]Lomonosov Moscow State University, Moscow, Russia

[4]Institute of Geography, RAS, Moscow, Russia

[5]NORCE Norwegian Research Centre, Bjerknes Centre for Climate Research, Bergen, Norway

[6]University of Copenhagen, Niels Bohr Institute, Denmark

[7]Department of Geography, University of Liège, Belgium

[8]Institut für Meereskunde, Universität Hamburg, Hamburg, Germany

[9]Max Planck Institute for Meteorology, Hamburg, Germany

[10]Environmental Meteorology, Faculty of Regional and Environmental Sciences, University of Trier, Germany

[11]Swedish Meteorological and Hydrological Institute, Norrköping, Sweden

[12]Bolin Centre for Climate Research, Stockholm University, Stockholm, Sweden

[13]Alfred Wegener Institute, Helmholtz Centre for Polar and Marine Research, AWI, Bremerhaven, Germany

[14]Centre ESCER, Université du Québec à Montréal, Montréal, Québec, Canada

[15]Danish Meteorological Institute, Copenhagen, Denmark

[16]Department of Physical Geography and Ecosystem Science, Lund University, 22362, Lund, Sweden

[17]Center for Permafrost (CENPERM), Department of Geosciences and Natural Resource Management, University of Copenhagen, Copenhagen, Denmark

[18]Institute of Applied Physics, Russian Academy of Sciences (Nizhny Novgorod, Russia)

[19]Centre for International Development and Environmental Research, Justus Liebig University Giessen, Germany

Keywords: Arctic, wind speed, wind energy, climate change, sea ice, biogeophysical feedback, surface roughness, regional climate models, ERA5, CORDEX

Corresponding author: Mirseid Akperov (aseid@ifaran.ru)

Preprint for publication in “Anthropocene”

Abstract

The Arctic has warmed more than twice the rate of the entire globe, a phenomenon known as Arctic amplification. Despite many negative impacts, a warmer Arctic could make the exploitation of renewable wind energy feasible. To quantify possible climate change effects, we calculate wind energy potentials from a multi-model ensemble of coordinated regional climate simulations from the WCRP-funded, Arctic-CORDEX initiative. For this, we analyze future changes of wind power density (WPD) using an eleven-member multi-model ensemble of Arctic-CORDEX simulations. Impacts are estimated for two periods (2020-2049 and 2070-2099) of the 21st century under a high emission scenario (RCP8.5).

The multi-model mean reveals an increase of seasonal WPD over the Arctic in the future decades. WPD variability across a range of temporal scales (from interannual to interdaily) is projected to increase over the Arctic. The signal amplifies by the end of 21st century. Future changes in the frequency of wind speeds at 100 m not useable for wind energy production (i.e. energy from wind flows with speeds below 4 m/s or above 25 m/s) has been analyzed. The RCM ensemble simulates a more frequent occurrence of 100m non-usable wind speeds for the current version of wind-turbines over Scandinavia and selected land areas in Alaska, northern Russia and Canada. In contrast, non-usable wind speeds decrease over large parts of Eastern Siberia and in northern Alaska. Thus, our results indicate increased potential of Arctic near-shore zones for the development and production of wind energy.

Bias corrected and not corrected near-surface wind and WPD changes have been compared with each other. It has been found that both show the same sign of future change, but differ in magnitude of these changes. The role of sea-ice retreat and vegetation expansion in the Arctic in future on wind speed variability has been also assessed. Surface roughness through sea-ice and vegetation changes may significantly impact on WPD variability in the Arctic.

1. Introduction

The Arctic warming in recent decades has proceeded at approximate twice the rate of the global mean temperature increase – locally more than four times the global rate - and is accompanied by an unprecedented reduction of sea ice extent (Jansen *et al.*, 2020; Rantanen *et al.*, 2022). These changes affect the weather in high latitudes and while retreating sea ice amplifies the warming, these changes result in an enhanced retreat of the sea ice cover in the Arctic Ocean (Vihma, 2014; Semenov and Latif, 2015). Retreating sea ice already allows better access by sea to the Arctic Ocean, which can be seen for marine shipping along the Northern Sea Route (Khon *et al.*, 2017; Kibanova *et al.*, 2018), may ease the extraction of oil and natural gas resources and increase the opportunities for renewable energy production in the Arctic off-shore zones (Pryor et al., 2020). However, all these activities will still be affected by, and indeed depend on, climate and weather conditions.

Investigating the spatial and temporal variability of near-surface wind speed is critical to assess the current wind energy potential and evaluate its future changes as the world continues to warm (Pryor *et al.*, 2005; Moemken *et al.*, 2018). The local near-surface wind speed variability is determined by large-scale, synoptic, and meso-scale circulations (storms, polar lows) as well as local conditions (Jakobson *et al.*, 2019). Large-scale atmospheric circulation patterns such as NAO/AO affect the cyclone activity in the Arctic (Akperov *et al.*, 2019) and impact on local wind characteristics (Laurila *et al.*, 2021). Polar mesocyclones or polar lows are associated with high wind speeds, especially over the Nordic Seas (Rasmussen, 2003). Local conditions, such as atmospheric stratification, sea ice concentration, topography or surface roughness (Akperov *et al.*, 2020), affect the spatial and temporal variability of the near-surface wind speed patterns. Therefore, quantifying the variability of the near-surface wind is of particular important for planning wind farms and safety at sea in general.

Future changes in wind resources were previously examined using data from CMIP5/6 (and respective downscalings from the CORDEX project) for various regions of the Northern Hemisphere under climate change scenarios (Hosking *et al.*, 2018; Li *et al.*, 2020; Carvalho *et al.*, 2021). Most of these studies focus on wind energy resources of specific countries and regions in the midlatitudes (Jung and Schindler, 2022). Due to the low density of the meteorological stations in the coastal zones of the Arctic, as well as in their absence, in particular on the shelf, there are very few or no assessment of regional wind energy resources available. The application of regional climate models (RCM) is one tool to assess the wind energy resources in the Arctic and project the impact of climatic changes on it. Compared to global climate models, RCMs with higher spatial resolution and more detailed surface processes may better capture the near-surface winds, especially in the Arctic (Gutjahr and Heinemann, 2018). Also as shown by Akperov *et al.* (2018), RCMs can capture cyclone activity and its variability in the Arctic more realistically than their driving GCMs. Therefore, we may expect better surface wind statistics associated with cyclone activity and local conditions by using RCMs. However, it should be noted that there are two well documented main sources of uncertainty associated with RCM assessments: 1) the choice of global climate model used for the boundary conditions; 2) the choice of the RCM itself. Therefore, the use of a multi-model ensemble consisting of different RCMs with different parameterizations and GCM-driven boundary conditions is necessary to assess the robustness of wind resource climate signals. In this study, we analyze an ensemble of Arctic-CORDEX RCMs (https://climate-cryosphere.org/polar-cordex/) to assess the sensitivity of wind resources in the Arctic to climate change.

Many different statistical bias correction techniques are implemented for reducing biases (Li *et al.*, 2019a). Overall, bias correction of climate projections is based on the comparison between observed and GCM/RCM-simulated variables. Very popular bias correction technique widely used in future climate analysis is quantile mapping (QM), which is based on correcting the shape of the entire variable distribution by establishing statistical relationships between cumulative density functions from the observed and simulated variable (Haas *et al.*, 2014a). We will assess the impact of bias correction on wind power density (WPD) changes.

The remainder of the manuscript is organized as follows. In Section 2 we discuss the datasets and methods. In Section 3, we review the model ensemble for consistency with a contemporary reanalysis product, ERA5 (Hersbach *et al.*, 2020) In Section 4, we assess the projected wind speeds and WPD changes in the 21st century. In Section 5, we assess uncertainties in WPD projected changes. Finally, we conclude in Section 6.

2. Data and Methods

2.1. Data

We analyze a set of 11 RCM simulations from six different RCMs, which have been driven by four different GCMs from CMIP5. See Table 1 for all details about the RCM-GCM matrix. Specifically, we analyze three-hourly 10 m wind data from an ensemble of six atmospheric RCMs (CRCM5, HIRHAM5-AWI, HIRHAM5-DMI, MAR3.6, RCA4, RCA-GUESS) from Arctic-CORDEX, driven by four different GCMs (NorESM1-M, CanESM2, MPI-ESM-LR, EC-EARTH) from CMIP5 and ERA5 reanalysis data (Table 1) for the Arctic region (Figure 1) for four seasons – winter (DJF), spring (MAM), summer (JJA) and autumn (SON). The GCMs provide lateral and lower boundary (sea surface temperature and sea ice fraction) forcing. The RCMs apply the Arctic CORDEX grid (rotated 0.44° x 0.44° degrees grid, 116 x 133 grid points).

All RCMs are atmospheric models coupled with land surface modules. This means that the RCMs are not constrained by surface conditions over land, e.g. each model calculates the time evolution independently from the driving model or ERA5. One of the models (RCA-GUESS) is, in addition, interactively coupled with the vegetation-ecosystem model LPJ-GUESS (Smith *et al.*, 2011; Zhang *et al.*, 2014). RCA-GUESS provides two runs, one with and the other without interactive vegetation–atmosphere coupling, hereinafter denoted as the feedback run (FB) and non-feedback run (NoFB), respectively. FB implements interactive vegetation dynamics in the land surface scheme for the entire simulation period (1961–2100), while NoFB uses fixed land surface properties representing the mean state for 1961-1990, which is similar to how the other RCMs treats the surface interactions. We interpret the difference "FB minus NoFB" as effects by biogeophysical feedbacks (Akperov *et al.*, 2021). More detailed information about the RCMs is available in Table 1.

The RCM simulations are driven by the four above-mentioned CMIP5 GCMs for a historical period (from 1950 to 2005) and for a scenario period (from 2006 to 2099) following the high emission scenario (RCP8.5) (Taylor *et al.*, 2012). We have chosen RCP8.5 because multi model data are available for this scenario, but not for others (https://climate-cryosphere.org/polar-cordex/). We note that a high end scenario also results in a strong climate response, reducing an additional source of uncertainty related to issues with a signal to noise ratio. We focus our analysis of future wind power density on the 30-year periods 1970-1999 as historical (reference) period and two periods (2020-2049 and 2070-2099) as future periods.

For comparing the RCM results with the reanalysis for the present-day (1980-2005), we use three-hourly 10 m wind data from the ERA5 reanalysis. The ERA5 data have been bilinearly interpolated onto the Arctic-CORDEX model grid for comparison.

2.2 Wind Power Density

The wind power density (WPD) is an important measure for assessing the potential of wind energy (Nikolaev et al., 2008; Emeis, 2013). It is defined as

$$WPD = \frac{1}{2}\rho u^3, \qquad (1)$$

where *u* is the wind speed at a given measurement height or adjusted-to-hub height (i.e., the traditional turbine operational height, here 100 m), and ρ is the air density (take as ~ 1.292 kg/m^3).

WPD is a measurement of the wind power that is available per unit turbine area (W/m^2). There are several methods commonly used to extrapolate near-surface wind speed measurements to the hub height. One is to use the power law method (Emeis, 2005; Pryor *et al.*, 2005; Hueging *et al.*, 2013; Tobin *et al.*, 2015), which assumes that wind speed at a certain height z is approximated by

$$u(z) = u(z_r)\left(\frac{z}{z_r}\right)^{\alpha}, \quad (2)$$

where z_r is the reference height, $u(z_r)$ is the wind speed at z_r and α is the power law exponent. In our case z_r is 10 m. Since RCMs do not provide wind speeds at 100m level as a standard output variable, but only at 10 m height, an extrapolation (such as in equation 2) is needed. However, α has to be known. This is particular critical in the Arctic with its complicated boundary layer structure (Lüpkes *et al.*, 2013). Since ERA5 also provides wind speeds at 100 m, analysis was made to obtain appropriate values of α. For this purpose, the available ERA5 100 m wind was compared to the extrapolated 100 m using the power-law equation. Finally, we found and applied the following values of α which minimize the differences between the extrapolated and original 100 m ERA5 winds: 0.18 for land, 0.08 for water and 0.12 for sea-ice grid points. For the surface condition classification we use the land-sea and sea-ice masks of the respective RCMs. It should be noted that this empirical extrapolation does not account for effects of atmospheric stability or local topography, such as low-level jets, which may play also a role for WPD, since the wind maximum is typically at 100-300m height (Tuononen *et al.*, 2015; Heinemann *et al.*, 2022).

We correct the biases for near-surface wind speeds in the model simulations using the Weibull distribution-based quantile mapping method (Haas *et al.*, 2014b; Moemken *et al.*, 2018; Li *et al.*, 2019b). The simulated, historical distributions of 3-hourly near-surface wind speed are mapped onto that from ERA5 in order to obtain the transfer function for the bias correction. This transfer function is applied both to the historical and scenario distributions of the wind speed to obtain the corrected fields. It should be also noted that the quantile mapping method based on Weibull distribution shows the best skills in bias reduction among other commonly used correction methods (Li *et al.*, 2019b).

Therefore, the bias-corrected 10 m wind speed u_{corr} can be calculated using the following expression:

$$u_{corr} = c_{era5}\left[-\ln\left(1-\left(1-e^{-\left(\frac{u_{model}}{c_{hist}}\right)^{k_{hist}}}\right)\right)\right]^{1/k_{era5}},(3)$$

where u_{model} is the 10 m wind speed from RCM, c and k are scale and shape parameters of the cumulative Weibull distribution for wind speeds from ERA5 reanalysis and from RCM for the historical period (hist). Historical shape and scale parameters are used for the correction of both historical runs and future projections for the computation of WPDs.

Finally, we analyze future changes in the frequency of wind speeds at 100 m not useable for wind energy production. These are very relevant for the wind energy exploitation industry since the current wind turbines cannot produce energy from wind flows with speeds below 4 m/s (called the cut-in speed) or above 25 m/s (cut-off speed) (Carvalho *et al.*, 2021). To assess these changes, the difference between the historical and future periods in the number of days per year with wind speeds at 100 m below/above these thresholds were analyzed.

3. Comparison of 10 m wind speeds from historical simulations and ERA5 reanalysis

The surface winds from ERA5 exhibit the best agreement amongst the modern reanalyses with in situ observations in midlatitudes and Arctic (Graham et al., 2019; Ramon *et al.*, 2019; Minola *et al.*, 2020) and are widely used for assessments of wind energy resources for the different areas (Lambin *et al.*, (n.d.); Olauson, 2018; Soares *et al.*, 2020). Furthermore, as previously noted, there is a lack of quality wind observations over most of the Arctic-CORDEX domain. Therefore, we use near-surface wind speeds from ERA5 as the reference data in our analysis. However, we are aware that all reanalysis data (incl. ERA5) have limitations in representing local conditions (Dörenkämper *et al.*, 2020; Gruber *et al.*, 2022).

Here we compare 10 m wind speeds climatology from the multi-ensemble mean of historical runs and ERA5 reanalysis for the period 1980-2005. Figure 1 shows the near-surface wind climatology from the ERA5 reanalysis and multi-model mean as well as their differences for the four seasons (DJF, MAM, JJA, and SOM) in the Arctic. For all four seasons, higher values of wind speed in the multi-model mean is seen over the continents and lower values over the Arctic Ocean compared to ERA5. In spite of quantitative differences, the Arctic-CORDEX models reproduce the spatial distribution of wind speed over the Arctic with maximum wind speed over the Nordic Seas (the region of highest cyclone activity) and minimum over the continents for all four seasons. To examine the performance of Arctic-CORDEX model runs to represent mean wind speeds with respect to ERA5, we apply Taylor diagrams (Figure 2). The spatial correlation coefficients (R) between the individual models and ERA5 reanalysis wind speed range from 0.59 (RCA-GUESS) to 0.93 (CRCM5-MPIC) for winter, from 0.52 (RCA-GUESS) to 0.92 (CRCM5-MPIC) for spring, from 0.47 (RCA-GUESS) to 0.91 (CRCM5-MPIC) for summer and from 0.6 (RCA-GUESS) to 0.93 (CRCM5-MPIC) for autumn.

Figure 3 shows intra-annual variability (standard deviation of wind speed across four seasons) of wind speed from ERA5 and multi-model mean. It reveals strong regionally different patterns for near-surface wind speed, in particular strong seasonality over ice-free ocean and weak over land and ice-covered Arctic.

Overall, the historical runs show substantial differences compared to the ERA5 reanalysis; these differences are most pronounced over areas of complex topography (East Greenland and Norwegian coasts, south Alaska) and may be associated with improvement of local topography and wind systems, such as katabatic winds in RCMs. But they can be also associated with biases from the driving GCMs, especially over the sea ice areas (which deviates substantially from the observed most prominently in the vicinity of the observed sea ice edge) and from the RCM physics. These biases influence the climate change signal, in particular wind speed thresholds, which are relevant for wind energy production. To estimate the impact of bias correction on near-surface wind and WPD changes, we performed the analysis both with and without bias correction technique. As shown in Figure 2, corrected 10 m wind speeds are very close to ERA5 for all seasons compared to the uncorrected data. However, the further analysis in section 4 focuses on not corrected wind and WPD changes, while in section 5, we assess the role of bias-correction on WPD and wind changes,

4. Future changes of wind speeds and wind power density

The future responses of WPD are analyzed for the RCP8.5 scenario run for the two periods (2020-2049 and 2070-2099). We investigate future changes of seasonal WPD, which could be important for the planning of future wind farms.

The projected changes of the seasonal WPD from the multi-model mean are presented in Figures 4 and 5. In winter and spring, the areas of the strong increase of WPD are located over the eastern Barents and Kara Seas which are related to the projected strong sea ice retreat in these marginal seas. Additionally, WPD increases in the Greenland and Chukchi Seas. However, WPD decreases over the Norwegian Sea and western Barents Sea. In summer and autumn, a strong increase of WPD is calculated over the northern Barents, Kara, and Greenland Seas and along Arctic near-shore zones as well as Arctic Ocean in 2070-2099. This is associated with projected strong sea-ice retreat there (Figure 5). Reduction of WPD is noted over the southern Barents Sea. It is noted that we calculate also a strong increase of WPD over the Arctic Ocean in winter in 2070-2099, irrespectively of small sea ice reduction and the related minimal warming in this area. According to Figure 6, for the end of the century, all models agree on the positive sign of WPD changes over the Arctic Ocean, including parts of Barents Sea, Greenland and Chukchi Seas, and along Arctic near-shore zones in all seasons and the negative sign in the ice-free Barents and Norwegian Seas in winter, spring and autumn.

Further, we analyze changes in the variability of WPD, ranging from intra-annual to inter-daily timescales. These timescales are of high importance for the production and operation of the energy system and the integration of wind energy into the energy system (Moemken *et al.*, 2018). The inter-daily timescales are relevant for the power system management and energy trading, and intra-annual to inter-annual timescales are important for resource assessments and the planning of backup and storage facilities.

The seasonal changes of WPD (as shown in Figures 4 and 5) lead to an ensemble mean amplification of the intra-annual variability of WPD (standard deviation of WPD across four seasons) over the Arctic Ocean and the Arctic near-shore regions (Figure 7). While in 2040-2060 the maximum increase is over the northern Barents, Kara, and Greenland Seas, in 2070-2099 the increase reaches up to 300 W/m^2 over the northern Barents-Kara and Chukchi Seas.

Changes in the inter-annual variability (standard deviation of annual WPD values in a given period) are presented in Figure 8. As for intra-annual variability, a remarkable increase of WPD is seen over the northern Barents-Kara, Greenland and Chukchi Seas by the end of 21st century. In contrast, a weak decrease is seen over the southern Barents Sea. Figure 9 shows the future projections for the inter-daily variability of WPD (standard deviation of averaged daily WPD values) for the model ensemble mean for the RCP8.5 scenario. Inter-daily variability of WPD also increases with remarkable changes over the northern Barents and Kara Seas, and Arctic near-shore regions by the end of the 21st century. However, there is a slight decrease over the Nordic Seas in both periods.

Figure 10 shows the projected changes in the number of occurrences of 3-hourly periods per year for the 100 m wind below cut-in (4 m/s) or above cut-off (25 m/s) speeds under the RCP8.5 scenarios. This range of wind speed represents the non-usable wind for the energy production for the current generation of wind turbines. According to Figure 10, the future climate projections show increased occurrences of non-usable wind speeds over Scandinavia and selected land areas in Alaska, northern Russia and Canada. A decrease of non-usable wind speeds is calculated over the large part of Eastern Siberia and in northern Alaska. In general, the changes amplify by the end of 21st century. On the other hand, there are no projected changes of non-usable wind speeds over the Arctic Ocean including Arctic near-shore zones where WPD increases in all seasons by the end of 21st century (Figure 4 and 5).

5 Uncertainties in WPD future changes

5.1 Bias correction

The sensitivity of WPD projections to the bias correction method is analyzed by calculating the difference between corrected and not corrected WPD changes (Costoya et al., 2020). Significant differences between corrected and not corrected WPD are seen in the ocean regions of strong WPD changes (Figures 4 and 5). WPD based on bias-corrected data are generally reduced compared to using non-corrected data. The reduction in WPD by using bias-corrected wind data can reach 50%. In winter and spring, the areas of strong differences between corrected and not corrected WPD are located in particular over the Barents-Kara, Greenland and Chukchi Seas. Also in summer and autumn, significant WPD differences occur over the Arctic Ocean including Arctic near-shore areas. These differences partly reflect the greater loss of sea ice in these sub-regions (see also sec. 5.2). The WPD differences over land are generally small, and show up especially over areas of complex terrain (e.g., Greenland and coastal regions). The inspection of the intra-annual, inter-annual and inter-daily WPD differences (Figures 7, 8 and 9) show that the bias-corrected data lead to an increase of the WPD variability. Overall, both bias-corrected and not corrected WPD changes show the same sign of future change, but differ in the magnitude of these changes.

Correction also impacts on future changes in the frequency of wind speeds at 100 m not usable for wind energy production. Figure 10 shows that remarkable changes are noticed over the areas of complex terrain. Corrected data shows a reduction of the frequency of non-usable wind speeds over the Alaska, Far East and other land areas over Russia. Increasing the frequency of non-usable wind speeds is seen over Scandinavia and over land areas in eastern Siberia.

5.2 Impact of surface conditions

One of the key factors influencing the near-surface wind in the Arctic in future is the sea ice reduction, which affects the aerodynamic surface roughness and stratification in the Arctic atmosphere. As was reported earlier (Mioduszewski *et al.*, 2018; Jakobson *et al.*, 2019; Vavrus and Alkama, 2021), reduction in ocean surface roughness caused by a transition from ice-covered to open water ocean and associated reduced atmospheric stability due the enhanced surface warming led to a strengthening of near-surface wind speeds in the Arctic. This, in turn, further affects the WPD changes. We confirm that the drastic sea ice loss in the Arctic including Arctic near-shore zones in all seasons by the end of 21st century (Figure 11) is associated with strong increase of WPD magnitude and variability over these areas (Figures 5, 7, 8, 9).

Regarding the land areas, Arctic warming changes, such as shrubification and the latitudinal and altitudinal shifts of tree-line, may change the fractional coverage of different vegetation types. This lead to a positive surface temperature feedback associated with lowered surface albedo and to a negative feedback associated with higher evapotranspiration (Eliseev and Mokhov, 2011; Pearson *et al.*, 2013; Zhang *et al.*, 2014, 2018). And this, in turn, leads to changes in static stability, atmospheric circulation through the changes in thermal meridional gradient and surface roughness through vegetation extent (Zhang *et al.*, 2014, 2018; Akperov *et al.*, 2021), and, therefore, may impact on near-surface wind speed and WPD changes over the land. Using RCA-GUESS simulations with and without interactive vegetation–atmosphere coupling, we assessed an impact of roughness changes (from vegetation expansion) on WPD. The strongest changes in near-surface air temperature are observed in spring and summer (Zhang *et al.*, 2014), therefore, both seasons have been chosen for the further analysis. Figure 12 shows spatial distribution of various variables between FB and NoFB simulations. The warming in spring and cooling in summer is in accordance to the above described feedbacks. Further, the vegetation changes (Arctic greening) over the land significantly impact on the near-surface wind speed as well as WPD in both seasons. The WPD is significantly reduced over the lands due to enhanced vegetation (increasing surface roughness). The reduction in WPD over the land by using changing vegetation can reach 100% (500 W/m^2 in spring and 250 W/m^2 in summer). These changes are comparable to those over the Arctic Ocean and exceed biases between not corrected and corrected WPD (Figure 5).

While WPD is reducing over the land in both seasons, static stability (which is expressed by the vertical difference in the temperature between 850 hPa and near-surface temperature) has a different behavior over the continents in spring and summer. In spring, static stability decreases, whereas it increases in summer. As was shown in (Akperov *et al.*, 2021), changing vegetation leads to a mean sea level pressure reduction (increase in cyclonicity which can lead to increased near-surface wind speed) over the continents in both seasons. Both factors should increase near-surface wind speed and WPD. However, near-surface wind speed decreases over the continents in both seasons (not shown).

Therefore, surface roughness through vegetation expansion on WPD variability over the continents may be seen as a key factor in controlling the wind speed.

We may conclude on significant uncertainties related to the estimation future changes in WPD. Both the sea-ice retreat and the vegetation expansion influence wind speed. At the same time using bias correction significantly changes the wind energy potentials in the Arctic in the future.

6. Summary and Conclusion

Our work presents an assessment of wind energy resources and associated spatiotemporal patterns over the Arctic using regional climate model simulations from the Arctic-CORDEX initiative within an RCP8.5 scenario for the 21st century. The multi-model mean projections reveal an increase of seasonal WPD over the Arctic in the future decades. In winter and spring, the areas of the strong increase of WPD are located over the eastern Barents, Kara, Greenland and Chukchi Seas. WPD decreases over the Norwegian Sea and western Barents Sea. In summer and autumn, WPD increases over the northern Barents, Kara, and Greenland Seas and along Arctic near-shore zones as well as Arctic Ocean in 2070-2099. The signals become stronger by the end of 21st century. However, increasing WPD variability in future decades will lead to a higher irregularity of wind energy production.

The RCM ensemble exhibits a more frequent occurrence of 100m non-usable wind speeds over Scandinavia, northern Russia, Canada and selected land areas in Alaska in the future climate. In contrast, non-usable wind speeds decrease over the large part of Eastern Siberia and in northern Alaska. All changes of the non-usable wind speeds occur over the land areas and away from the coastal zone.

We quantify the sensitivity of WPD projections to the bias correction by calculating the difference between bias-corrected and not corrected WPD changes. The reduction in WPD by using bias-corrected wind data can reach 50%. The areas of strong differences between bias-corrected and not corrected WPD are located over the WPD seasonal increase and decrease. Overall, because both corrected and not corrected WPD changes show the same sign of future change the sign of the response in our paper is credible. However, the respective magnitude remains uncertain. We note, however, that bias correction (as well as any statistical post-processing procedure) is unlikely able to improve possible model shortcomings in projecting a non-linear response of wind to climate forcing. On the other hand, some credibility for our results is provided by the absence of such nonlinear response in large-scale forcing data.

The role of sea-ice retreat and vegetation expansion on near-surface wind speed and WPD variability has been also assessed. Reduction in ocean surface roughness caused by a transition from ice-covered to open water and reduced atmospheric stability and greater vertical momentum mixing due the enhanced surface warming lead to strengthening near-surface wind speeds over the Arctic with the most pronounced effect in winter-autumn. Similarly, the near-surface wind speed as well as WPD significantly decreases over the continents due to increasing vegetation extent (surface roughness) in biogeophyscial feedback simulations in spring-summer.

Estimations of the future WPD changes suffer from different kinds of uncertainty. These are related to changes of the air density, which is expected to decrease due to near-surface temperature increase. Especially, it is expected to have an effect over the Barents Sea (Koenigk *et al.*, 2013). However, a contribution of air density changes to WPD will be much smaller compared to changes in near-surface wind speeds. Other uncertainties are related to the height of future wind turbines, which is expected to be higher than the current generation of turbines (McKenna *et al.*, 2016), and - although not addressed in this work – to the considered emission scenario.

Since the worst (the highest emission) scenario RCP8.5 provides some sort of upper estimate of possible changes and since the largest number of CORDEX simulations were available for RCP8.5, we analyzed this scenario to highlight the possibly strongest changes possible by the end of the 21st century, in frame of the commonly accepted concept of the anthropogenic climate change (e.g. IPCC, 2021). Again, we note that the results of low (RCP2.6) and high emission scenarios are very similar for the near future of two-three decades – but differ substantially for the end of the 21st century.

We note that the CMIP5/6 ensemble of GCMs appear to be biased when it comes to the retreat of Arctic sea ice (Massonnet *et al.*, 2012; Collins *et al.*, 2013; Koenigk *et al.*, 2015; Eliseev and Semenov, 2016; Docquier and Koenigk, 2021) In particular, it has been demonstrated that future scenarios of sea ice retreat building on CMIP5 only match current rates of Arctic change in GCMs following a scenario with greater warming than RCP4.5, with few exceptions (Jansen et al., 2020). The current suite of driving GCMs has not been chosen with this in mind, which may imply that even end of century projection of WPD may be better captured using RCP8.5 than lower emission scenarios even if greenhouse gas emissions would stay below the emission levels assumed by RCP8.5.

Overall, this study provides state-of-the-art information on wind power characteristics over the Arctic based on a recent ensemble of regional climate model simulations (Arctic-CORDEX). Of course, reducing uncertainties in projections due to reduced model biases could greatly benefit future investigations, including those improvements in representing wind speeds that may arise from higher horizontal resolution. Improvements in in-situ observational coverage and monitoring of wind speed will help in this regard and are sorely needed. Also, temporal, seasonal, and geographical variations in climatic characteristics (such as sea ice decrease, surface roughness, scenario changes) may introduce some uncertainty into such projections. Nonetheless, the global long-term transition to renewable energy sources for environmental sustainability means that the results of this study are vital. Detailed projections of changes in wind speed and WPD are crucial for the development and sustainability of not only wind power systems, but also energy supply, that is necessary in order to prevent energy crises. Therefore, the improvement in climate models (ranging from improved model physics to better representation of local conditions in the Arctic) may allow a more robust projection of wind energy potential.

Acknowledgements

The development and implementation of the bias correction scheme were supported by the Russian Science Foundation (RSF № 21-17-00012). WPD analysis was supported by the Russian Science Foundation (RSF № 23-47-00104). Wind speed analysis was supported by the Russian Science Foundation (RSF № 19-17-00240). The analysis of predicted changes of WPD was supported by Russian Ministry of Science and Higher Education (Agreement №. 075-15-2021-577) and partly supported by Russian Center of Scientific Information№. 20-55-14003. DS was supported by the Germany-Sino Joint Project (ACE, No. 2019YFE0125000 and 01LP2004A) and the SIO RAS State

Assignment (№ FMWE-2021-0014). AR and HM were partly supported by the European Union’s Horizon 2020 research and innovation framework programme under Grant agreement no. 101003590 (PolarRES) and 869471 (CHARTER). WZ was supported by the grants from Swedish Research Council VR (2020–05338) and Swedish National Space Agency (209/19). This study is a contribution to the strategic research areas Modeling the Regional and Global Earth System (MERGE) at Lund University.

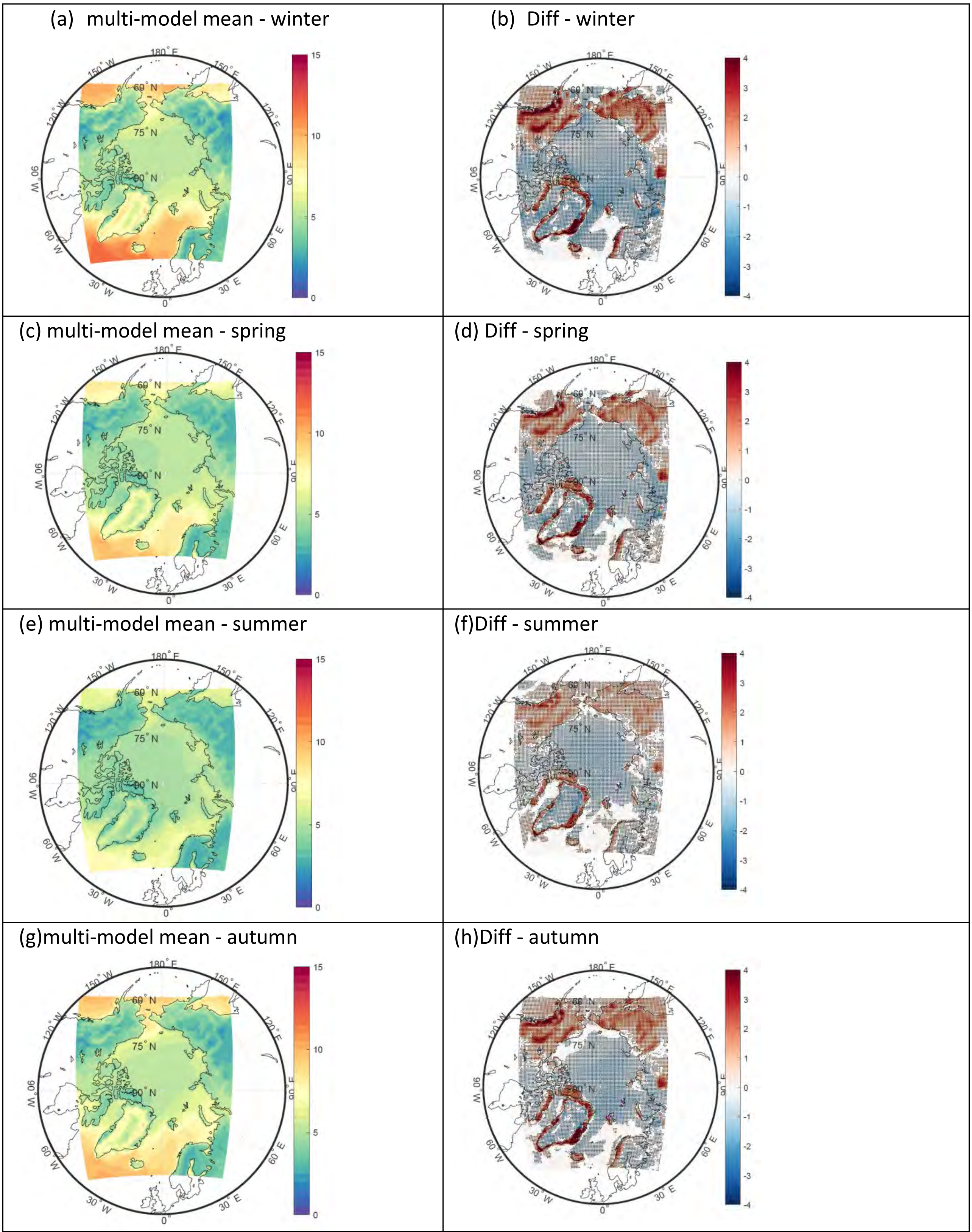

Figure 1 Climatological mean of 10 m wind speed in m/s for multi-model mean for the 1980-2005 for the different seasons and their differences (‘multi-model mean’ – ‘ERA5’). Black dots indicate statistical significance ($p < 0.05$).

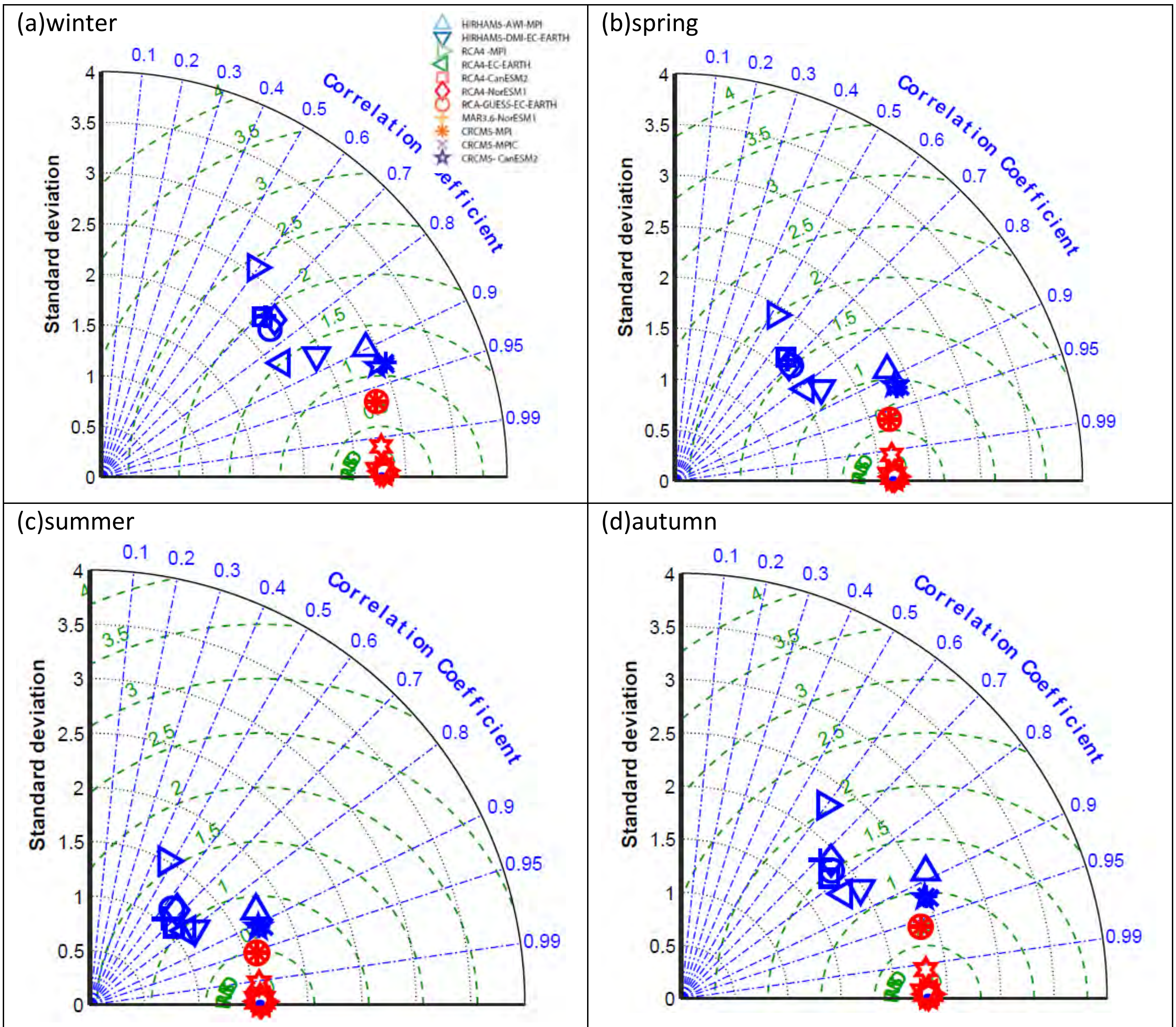

Figure 2 Taylor diagrams of seasonal mean wind speeds (m/s) from spatially averaged data for ERA5 (reference data) and Arctic-CORDEX simulations 2005 for the corrected (red) and not corrected (blue) data temporally averaged during 1980-2005.

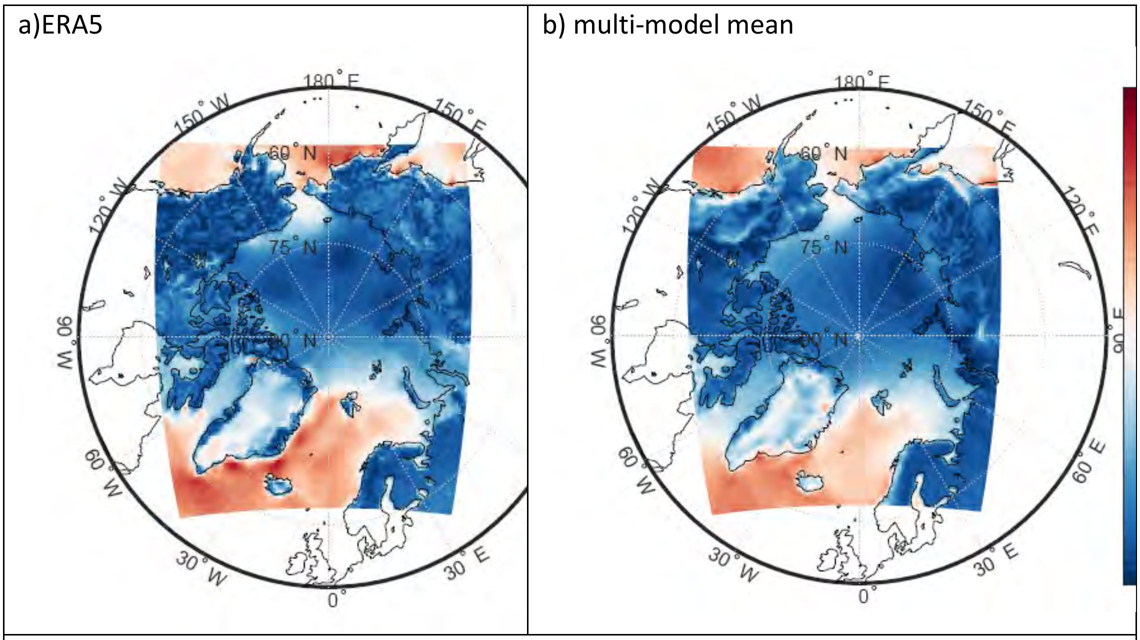

Figure 3 Intraannual variability of wind speed (m/s) of ERA5 (a) and multi-model mean (b).

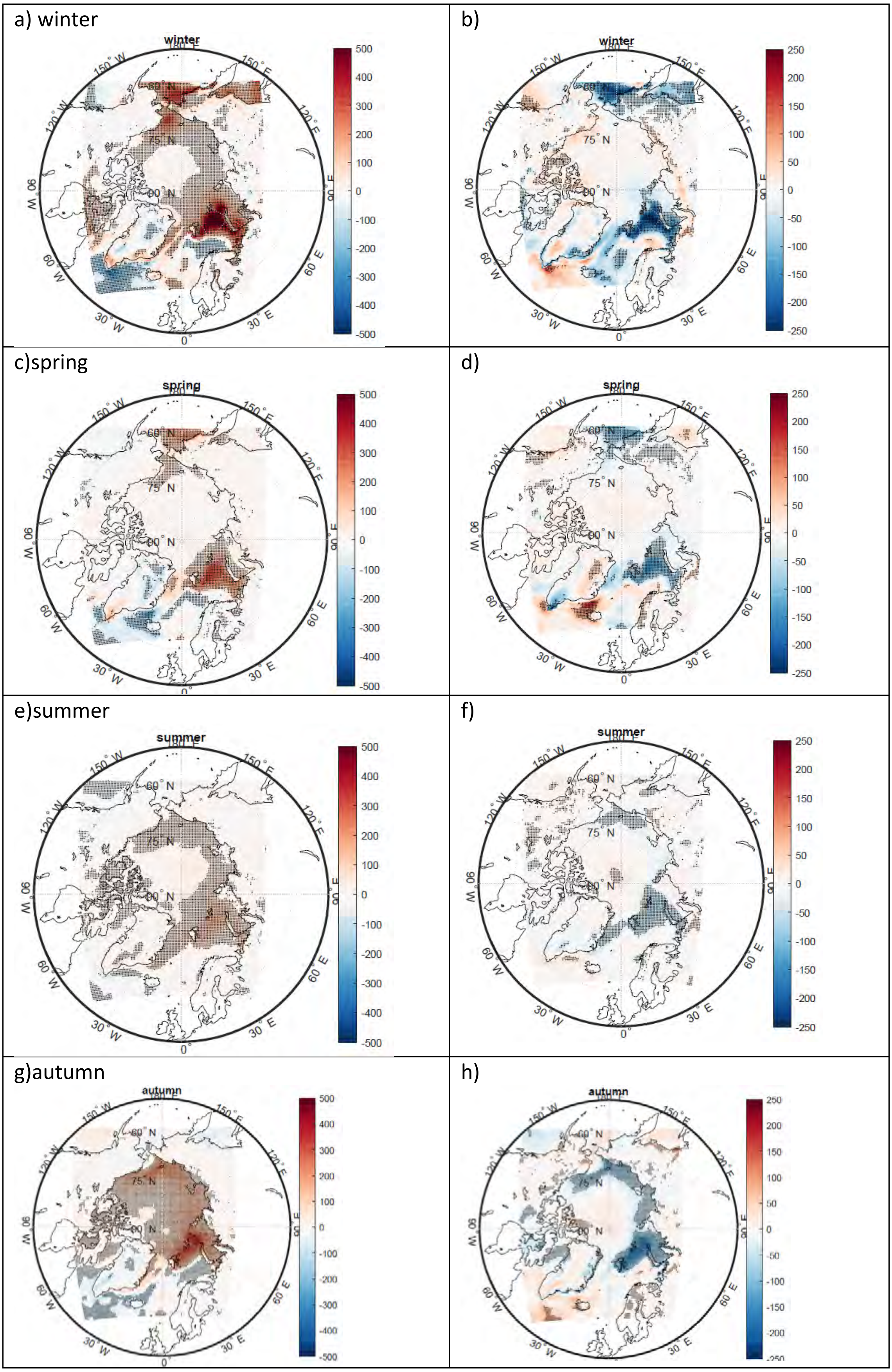
a) winter
b)
c)spring
d)
e)summer
f)
g)autumn
h)
winter
spring
summer
autumn
60° N
75° N
90° N
150° W
120° W
90° W
60° W
30° W
0°
30° E
60° E
90° E
120° E
150° E
500
400
300
200
100
0
-100
-200
-300
-400
-500
250
200
150
100
50
0
-50
-100
-150
-200
-250

Figure 4 Changes of seasonal WPD (W/m2) for the multi-model mean of RCP8.5 (2020-2049) with respect to historical period (1970-1999) (a,c,e,g) and differences between bias-corrected and not corrected WPD for the corresponding seasons (b,d,f,h).

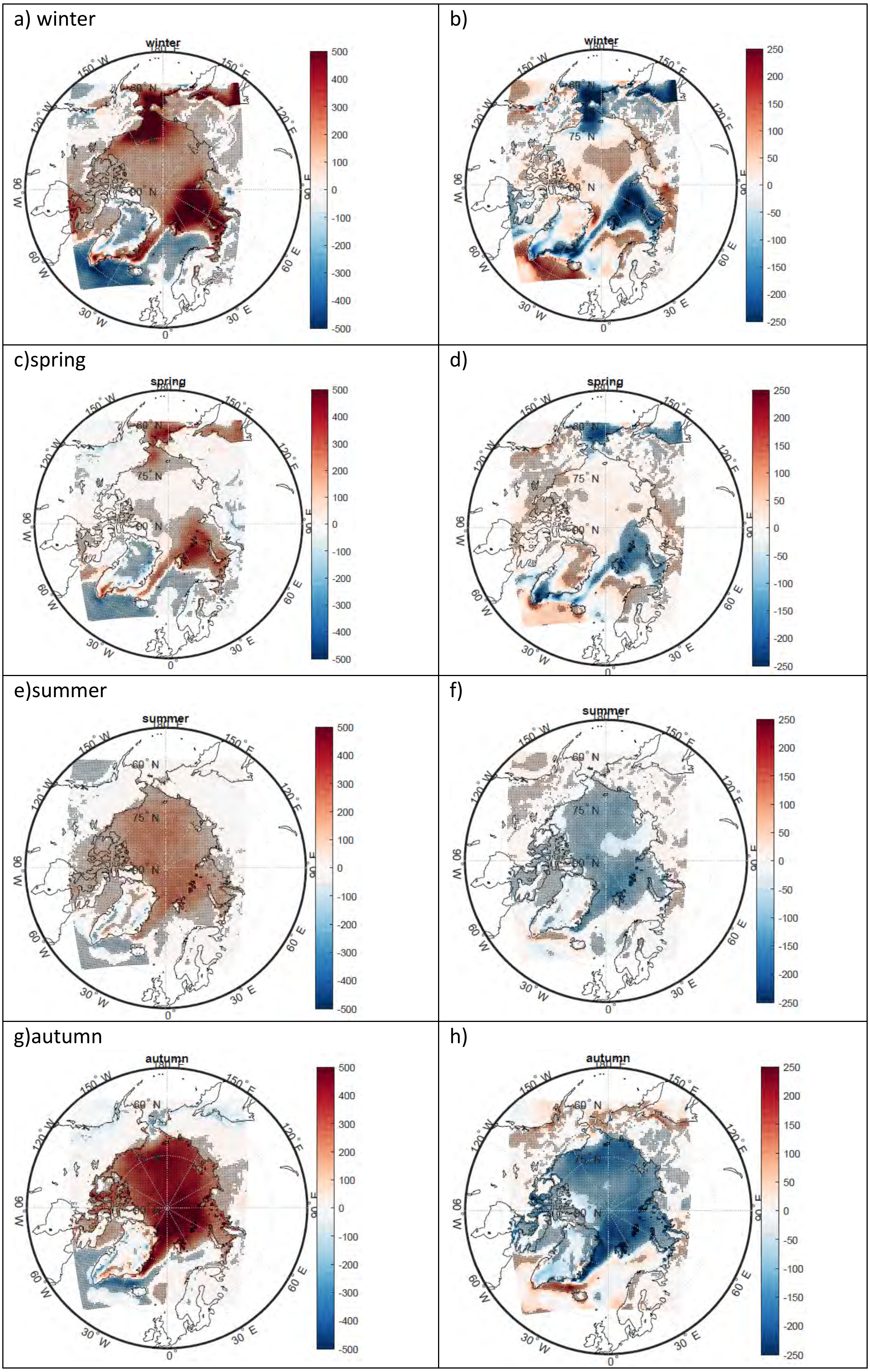

a) winter
b)
c)spring
d)
e)summer
f)
g)autumn
h)
winter
spring
summer
autumn
500
400
300
200
100
0
-100
-200
-300
-400
-500
250
200
150
100
50
0
-50
-100
-150
-200
-250
150° W
150° E
120° W
120° E
90° W
90° E
60° W
60° E
30° W
30° E
0°
60° N
75° N

Figure 5 Changes of seasonal WPD (W/m^2) for the multi-model mean of RCP8.5 (2070-2099) with respect to historical period (1970-1999) (a,c,e,g) and differences between bias-corrected and not corrected WPD for the corresponding seasons (b,d,f,h).

507

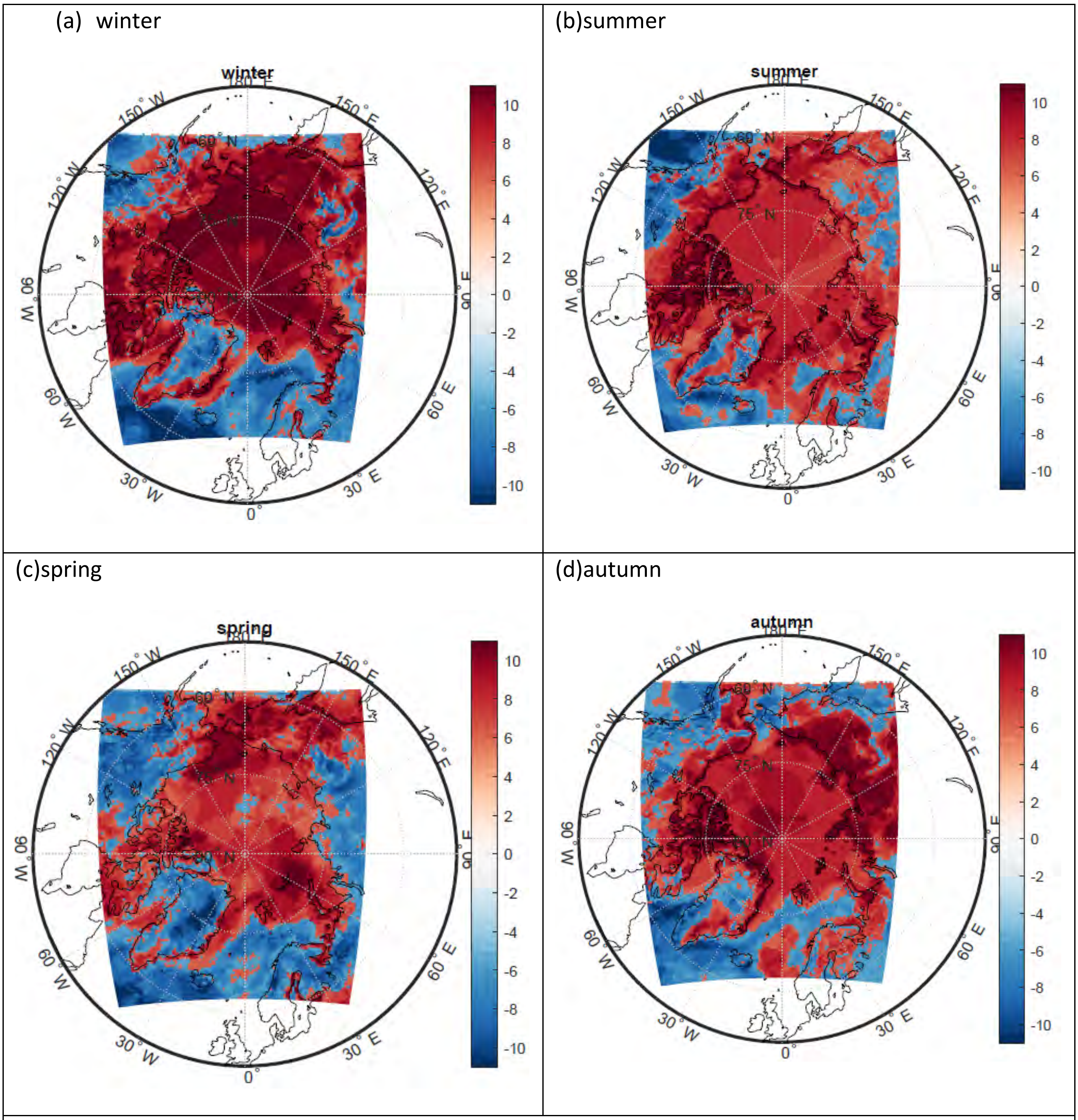

Figure 6 Number of Arctic-CORDEX not corrected models showing positive or negative changes of WPD (W/m^2) for the period 2070-2099.

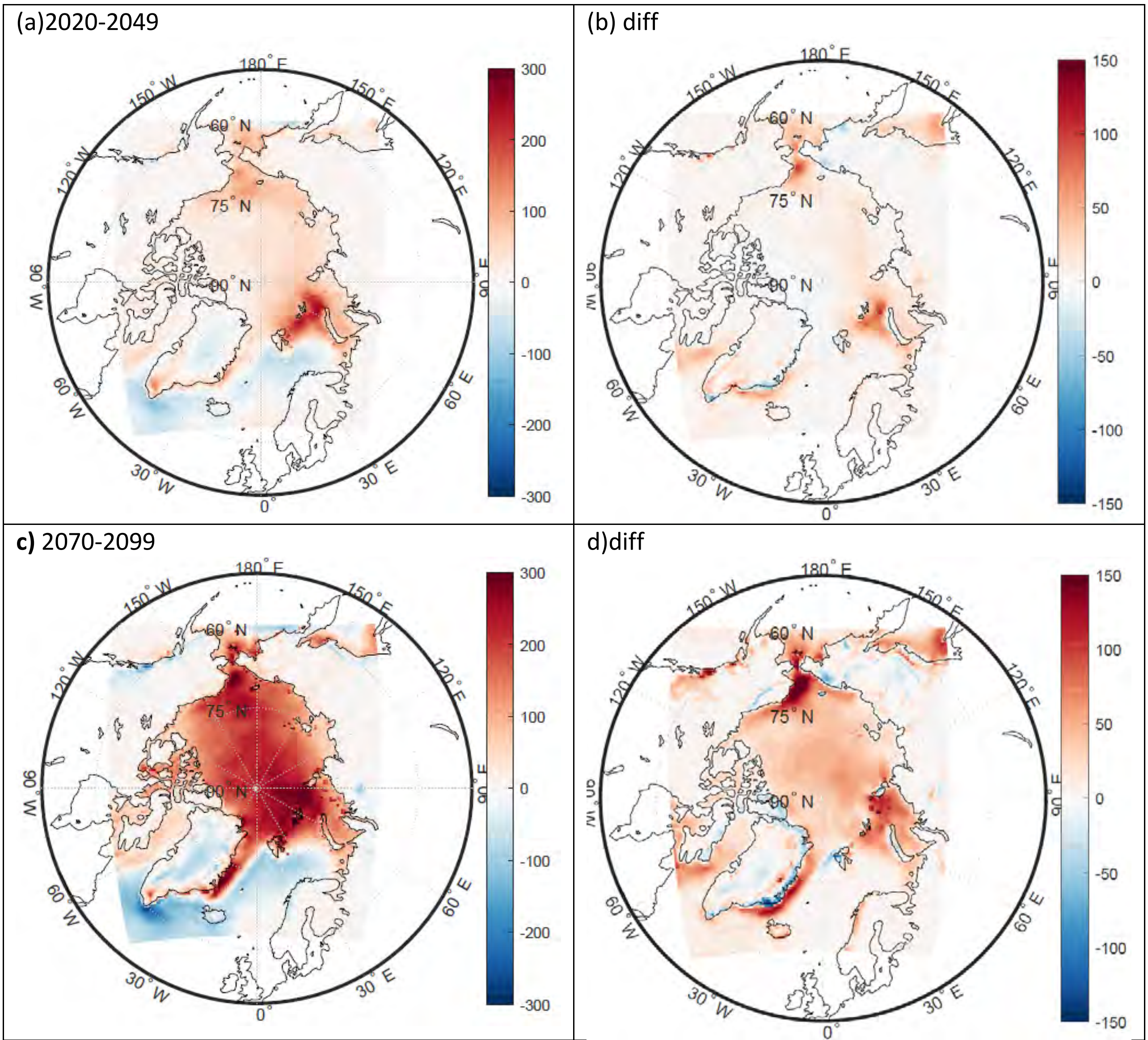

Figure 7 Changes of intra-annual variability of WPD (W/m^2) for the multi-model mean of RCP8.5 for the two periods (2020-2049 and 2070-2099) with respect to historical period (1970-1999) (a,c) and differences between bias-corrected and not corrected WPD for the corresponding figures (b,d).

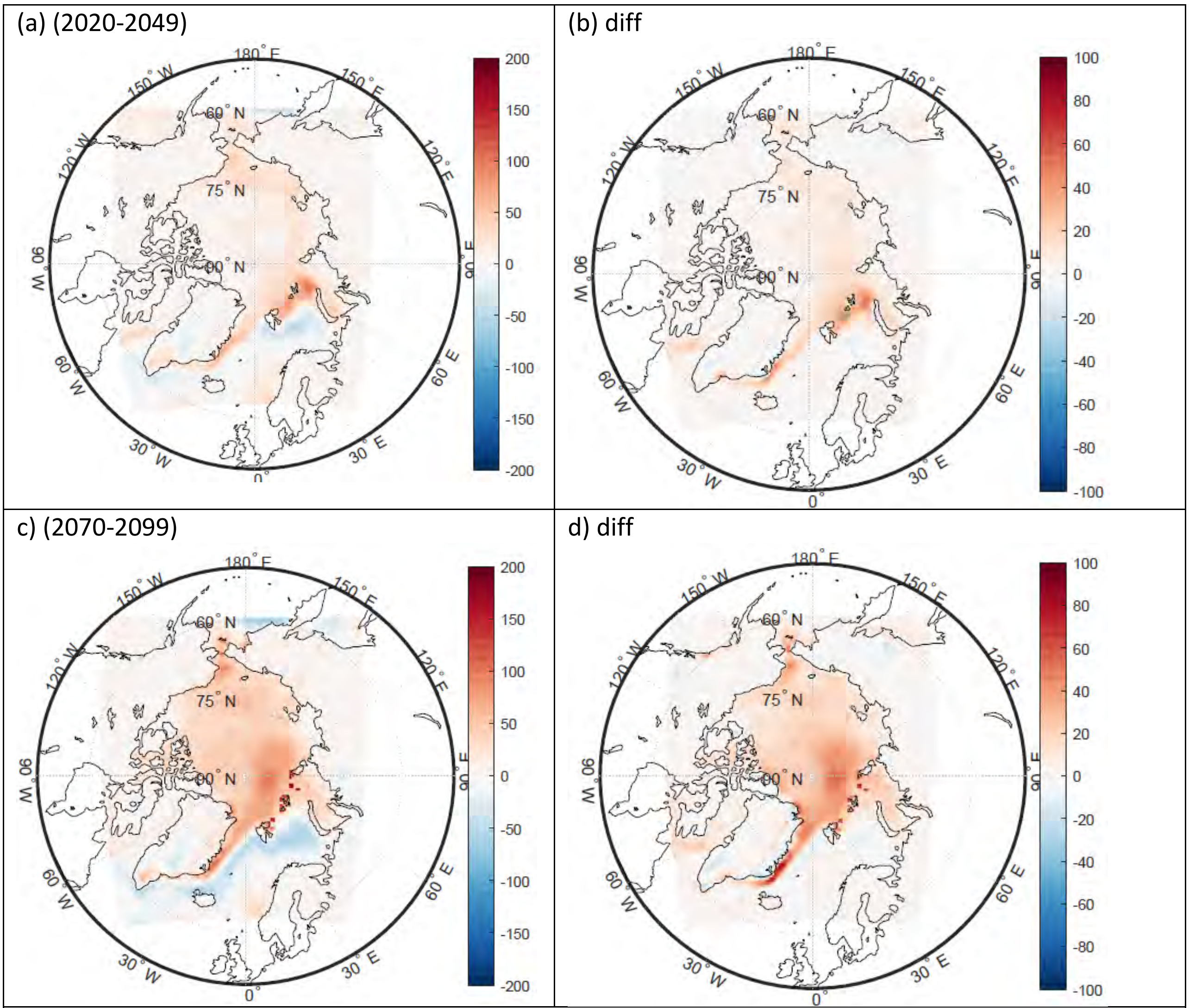

Figure 8 Changes of inter-annual variability of WPD (W/m^2) for the multi-model mean of RCP8.5 for the two periods (2020-2049 and 2070-2099) with respect to historical period (1970-1999) (a,c) and differences between bias-corrected and not corrected WPD for the corresponding figures (b,d).

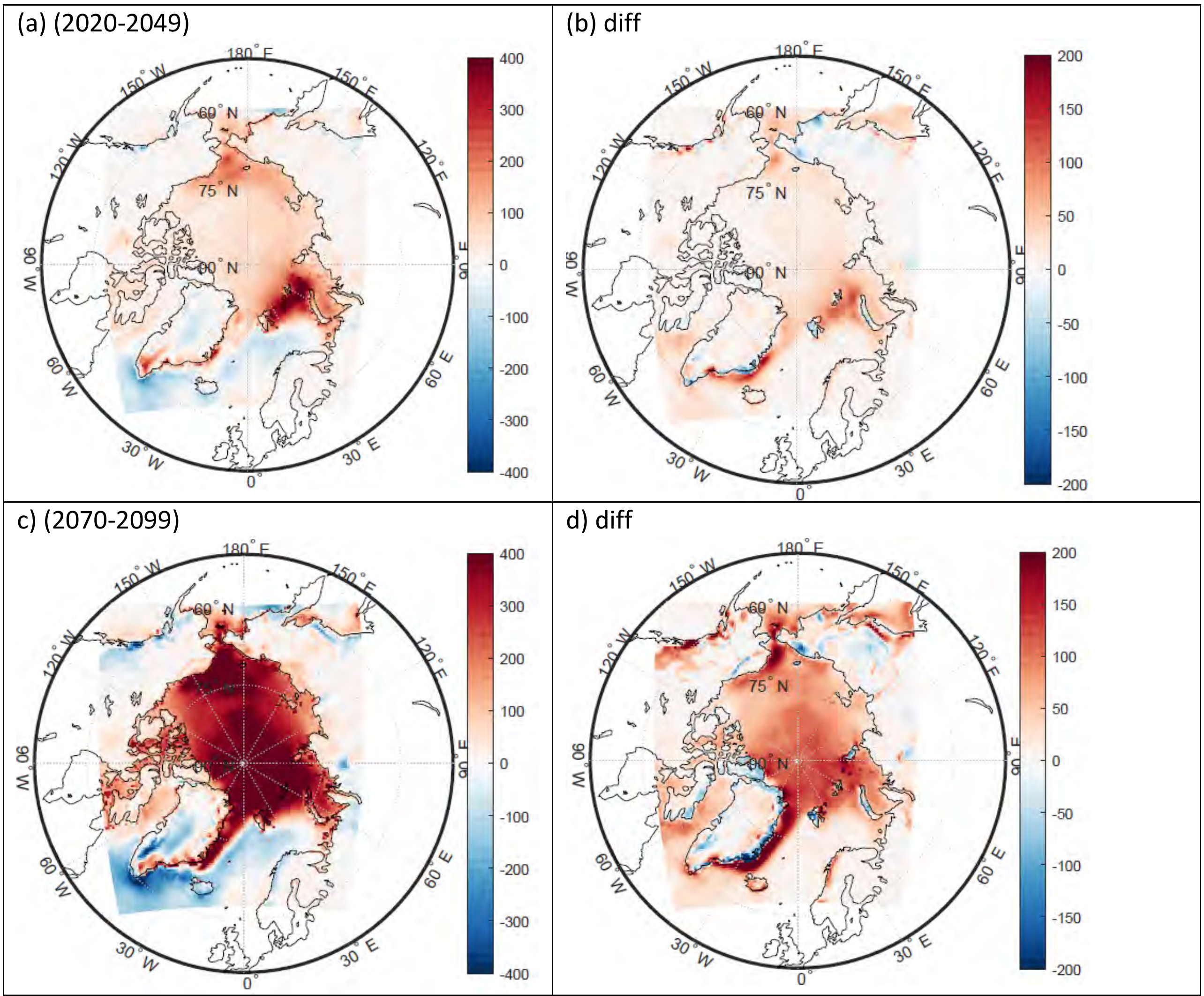

Figure 9 Changes of inter-daily variability of WPD (W/m^2) for the multi-model mean of RCP8.5 for the two periods (2020-2049 and 2070-2099) with respect to multi-model mean of historical (1970-1999) (a,c) and differences between bias-corrected and not corrected WPD for the corresponding figures (b,d).

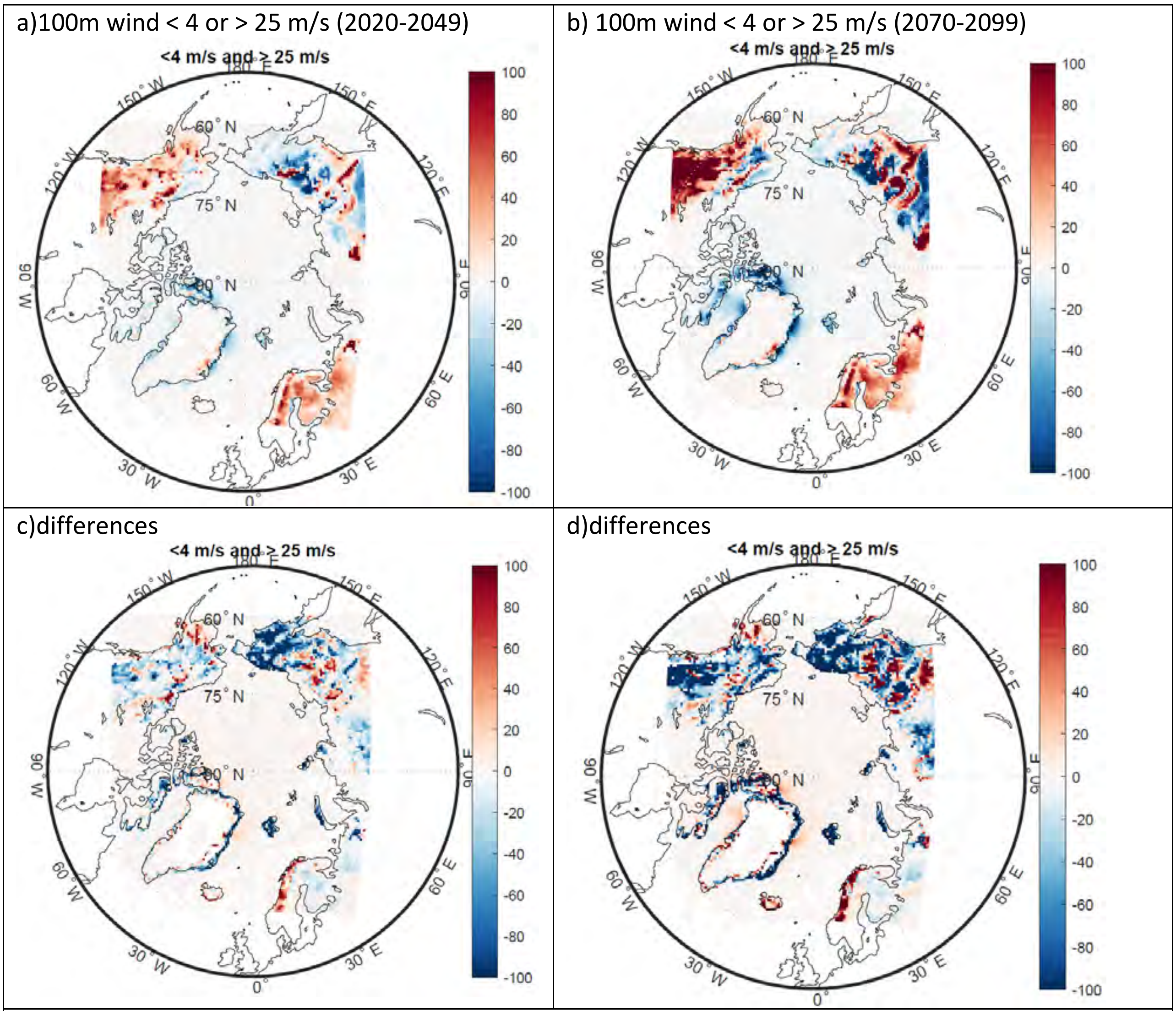

Figure 10 Changes in the number of three-hourly dates per year with (a,b) 100m wind speed < 4 or > 25 m/s from the multi-model mean of RCP8.5 for the two periods (2020-2049 and 2070-2099) with respect to multi-model mean of historical (1970-1999) and differences between bias-corrected and not corrected WPD for the corresponding figures (c,d).

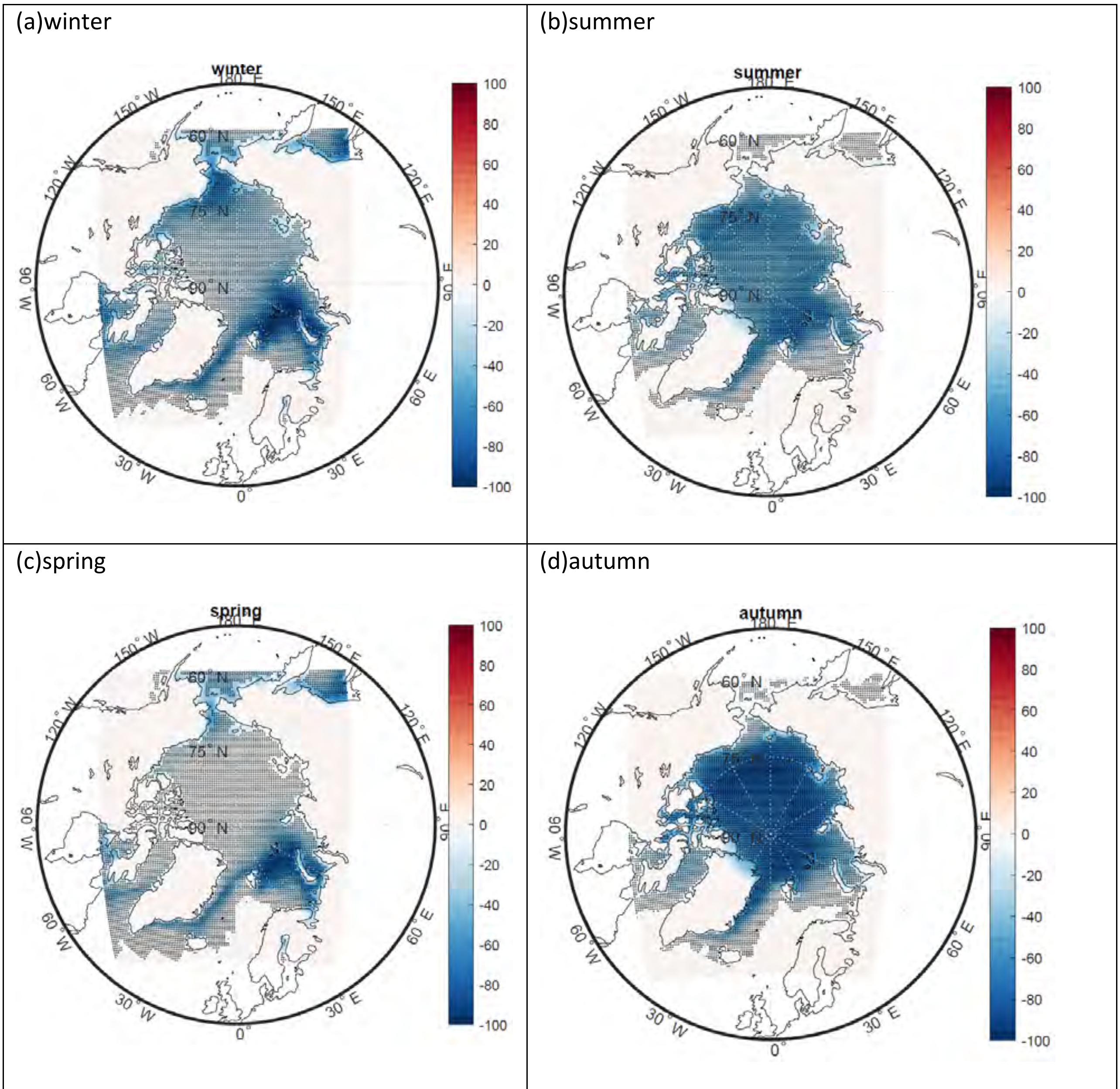

Figure 11 Changes in sea-ice concentration (%) for the multi-model mean of driving GCM's for RCP8.5 for the 2070-2099 with respect to multi-model mean of historical period (1970-1999) for the different seasons. Black dots indicate statistically significant differences ($p < 0.05$).

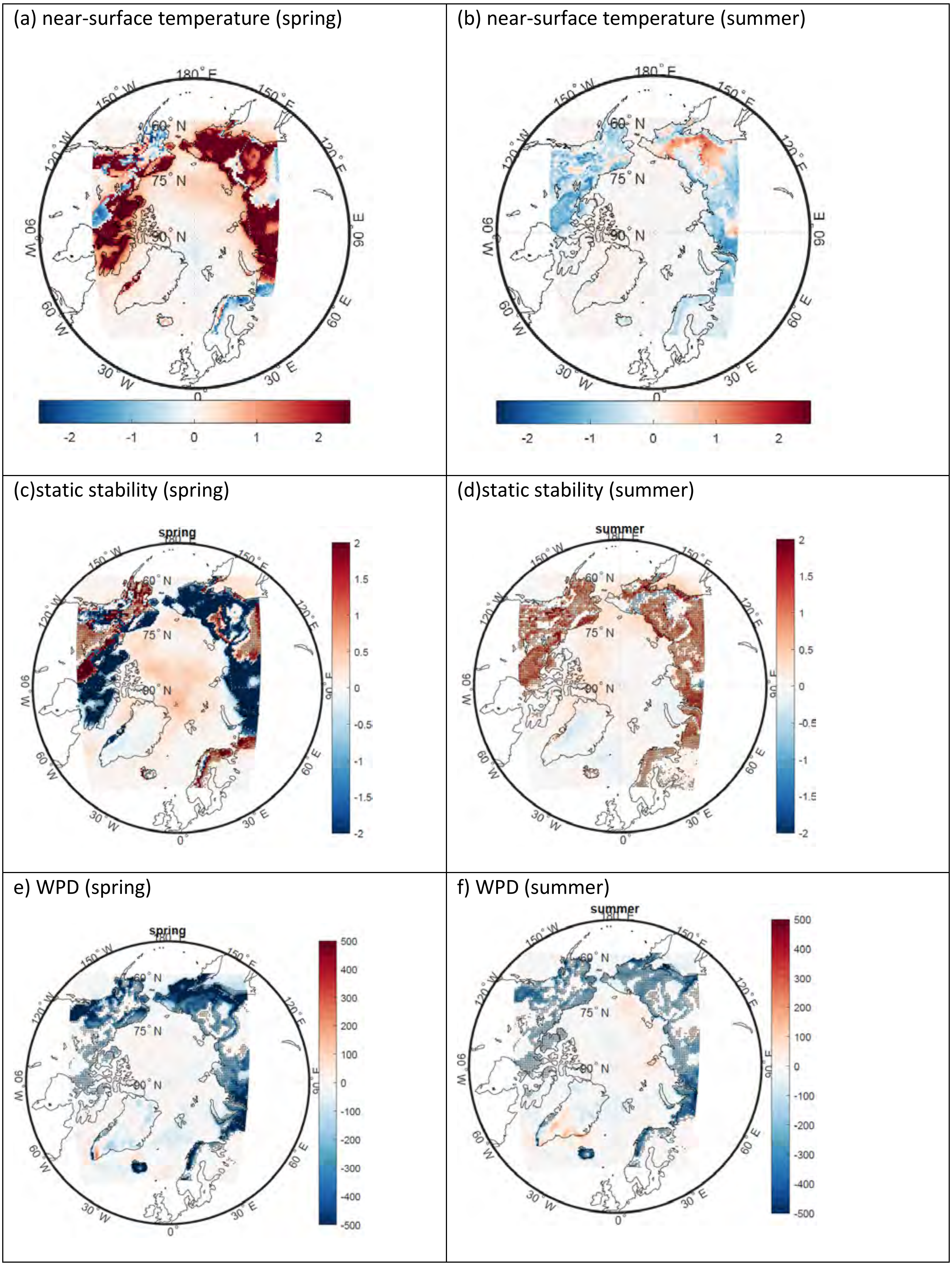

(a) near-surface temperature (spring)
(b) near-surface temperature (summer)
(c)static stability (spring)
(d)static stability (summer)
e) WPD (spring)
f) WPD (summer)
spring
summer
180° E
150° W
150° E
120° W
120° E
90° W
90° E
60° W
60° E
30° W
30° E
0°
60° N
75° N
90° N
-2
-1
0
1
2
1.5
0.5
-0.5
-1.5
500
400
300
200
100
-100
-200
-300
-400
-500

Figure 12 The effects of biogeophysical feedbacks on near-surface temperature [K] (a,b), static stability [K] (c,d) and WPD [W/m^2] (e,f) for the different seasons averaged from 2070 to 2099 with respect to historical period (1970-1999) in the RCP8.5 scenario. Black dots indicate statistically significant differences ($p < 0.05$).

Table 1. Reanalysis and regional climate models (RCMs), and their corresponding information.

Type	Institution/Country	Data/ Model name	Original Resolution Vertical levels, horizontal resolution	Boundary conditions	Reference
Reanalyses	ECMWF/UK	ERA5	L137, 0.28^0 (~ 30 km)		(Hersbach *et al.*, 2020)
Regional climate models (RCMs)	AWI/Germany	HIRHAM5-AWI-MPI	L40, 0.5^0 (~56 km)	MPI-ESM-LR	(Christensen and Christensen, 2007; Sommerfeld *et al.*, 2015; Klaus *et al.*, 2016)
	DMI/Denmark	HIRHAM5-DMI-EC-EARTH	L31, 0.44^0 (~48 km)	EC-EARTH2.3	(Christensen and Christensen, 2007; Lucas-Picher *et al.*, 2012)
	SMHI/Sweden	RCA4 -MPI	L40, 0.44^0, (~48 km)	MPI-ESM-LR	(Berg *et al.*, 2013; Koenigk *et al.*, 2015)
		RCA4-EC-EARTH		EC-EARTH2.3	

		RCA4-CanESM2		CanESM2	
		RCA4-NorESM1		NorESM1-M	
	LU/Sweden	RCA-GUESS-EC-EARTH	L40, 0.44^0, (~48 km)	EC-EARTH2.3	(Smith *et al.*, 2011; Zhang *et al.*, 2014)
	ULg/Belgium	MAR3.6-NorESM1	L23, 50 km (~0.5^0)	NorESM1-M	(Fettweis *et al.*, 2017)
	UQAM/Canada	CRCM5-MPI	L55, 0.44^0, (~48 km)	MPI-ESM-LR	(Martynov *et al.*, 2013; Šeparović *et al.*, 2013; Takhsha *et al.*, 2017)
		CRCM5-MPIC		MPI-ESM-LR (Bias correction)	
		CRCM5-CanESM2		CanESM2	
Global climate models (GCMs)	MPI/Germany	MPI-ESM-LR	L47, 1.8^0 (~200 km)		(Giorgetta *et al.*, 2013)
	ICHEC/EU	EC-EARTH	L62, 1.1^0 (~122 km)		(Hazeleger *et al.*, 2012)

	CCCma/Canada	CanESM2	L35, 2.8^0 (~310 km)		(Arora *et al.*, 2011)
	NCC/Norway	NorESM1-M	L26, 2.5^0 (~277 km)		(Bentsen *et al.*, 2013)

References

Akperov M, Rinke A, Mokhov II, Matthes H, Semenov VA, Adakudlu M, Cassano J, Christensen JH, Dembitskaya MA, Dethloff K, Fettweis X, Glisan J, Gutjahr O, Heinemann G, Koenigk T, Koldunov N V., Laprise R, Mottram R, Nikiéma O, Scinocca JF, Sein D, Sobolowski S, Winger K, Zhang W. 2018. Cyclone Activity in the Arctic From an Ensemble of Regional Climate Models (Arctic CORDEX). *Journal of Geophysical Research: Atmospheres*, 123(5): 2537–2554. https://doi.org/10.1002/2017JD027703.

Akperov M, Rinke A, Mokhov II, Semenov VA, Parfenova MR, Matthes H, Adakudlu M, Boberg F, Christensen JH, Dembitskaya MA, Dethloff K, Fettweis X, Gutjahr O, Heinemann G, Koenigk T, Koldunov NV, Laprise R, Mottram R, Nikiéma O, Sein D, Sobolowski S, Winger K, Zhang W. 2019. Future projections of cyclone activity in the Arctic for the 21st century from regional climate models (Arctic-CORDEX). *Global and Planetary Change*, 182. https://doi.org/10.1016/j.gloplacha.2019.103005.

Akperov M, Semenov VA, Mokhov II, Dorn W, Rinke A. 2020. Impact of Atlantic water inflow on winter cyclone activity in the Barents Sea: insights from coupled regional climate model simulations. *Environmental Research Letters*. IOP Publishing, 15(2): 24009. https://doi.org/10.1088/1748-9326/ab6399.

Akperov M, Zhang W, Miller PA, Mokhov II, Semenov VA, Matthes H, Smith B, Rinke A. 2021. Responses of Arctic cyclones to biogeophysical feedbacks under future warming scenarios in a regional Earth system model. *Environmental Research Letters*. IOP Publishing, 16(6): 64076. https://doi.org/10.1088/1748-9326/ac0566.

Arora VK, Scinocca JF, Boer GJ, Christian JR, Denman KL, Flato GM, Kharin V V, Lee WG, Merryfield WJ. 2011. Carbon emission limits required to satisfy future representative concentration pathways of greenhouse gases. *Geophysical Research Letters*. John Wiley & Sons, Ltd, 38(5): n/a-n/a. https://doi.org/10.1029/2010GL046270.

Bentsen M, Bethke I, Debernard JB, Iversen T, Kirkevåg A, Seland Ø, Drange H, Roelandt C, Seierstad IA, Hoose C, Kristjánsson JE. 2013. The Norwegian Earth System Model, NorESM1-M – Part 1: Description and basic evaluation of the physical climate. *Geoscientific Model Development*, 6(3): 687–720. https://doi.org/10.5194/gmd-6-687-2013.

Berg P, Döscher R, Koenigk T. 2013. Impacts of using spectral nudging on regional climate model RCA4 simulations of the Arctic. *Geoscientific Model Development*, 6(3): 849–859. https://doi.org/10.5194/gmd-6-849-2013.

Carvalho D, Rocha A, Costoya X, deCastro M, Gómez-Gesteira M. 2021. Wind energy resource over Europe under CMIP6 future climate projections: What changes from CMIP5 to CMIP6. *Renewable and Sustainable Energy Reviews*, 151(July). https://doi.org/10.1016/j.rser.2021.111594.

Christensen JH, Christensen OB. 2007. A summary of the PRUDENCE model projections of changes in European climate by the end of this century. *Climatic Change*, 81(SUPPL. 1): 7–30. https://doi.org/10.1007/s10584-006-9210-7.

Collins M, Knutti R, Arblaster J, Dufresne J-L, Fichefet T, Friedlingstein P, Gao X, Gutowski WJ, Johns T, Krinner G, Shongwe M, Tebaldi C, Weaver AJ, Wehner MF, Allen MR, Andrews T, Beyerle U, Bitz CM, Bony S, Booth BBB. 2013. Long-term Climate Change: Projections, Commitments and Irreversibility. In: Stocker TF, Qin D, Plattner G-K, Tignor MMB, Allen SK, Boschung J, Nauels A, Xia Y, Bex V and Midgley PM (eds) *Climate Change 2013 - The Physical Science Basis*. Cambridge University Press: United Kingdom, 1029–1136.

Docquier D, Koenigk T. 2021. Observation-based selection of climate models projects Arctic ice-free summers around 2035. *Communications Earth & Environment*, 2(1): 144. https://doi.org/10.1038/s43247-021-00214-7.

Dörenkämper M, Olsen BT, Witha B, Hahmann AN, Davis NN, Barcons J, Ezber Y, Garc\'\ia-Bustamante E, González-Rouco JF, Navarro J, Sastre-Marugán M, Sīle T, Trei W, Žagar M, Badger J, Gottschall J, Sanz Rodrigo J, Mann J. 2020. The Making of the New European Wind Atlas -- Part 2: Production and evaluation. *Geoscientific Model Development*, 13(10): 5079–5102. https://doi.org/10.5194/gmd-13-5079-2020.

Eliseev A V., Mokhov II. 2011. Uncertainty of climate response to natural and anthropogenic forcings due to different land use scenarios. *Advances in Atmospheric Sciences*, 28(5): 1215–1232. https://doi.org/10.1007/s00376-010-0054-8.

Eliseev A V, Semenov VA. 2016. Arctic climate changes in the 21st century: Ensemble model estimates accounting for realism in present-day climate simulation. *Doklady Earth Sciences*, 471(1): 1183–1187. https://doi.org/10.1134/S1028334X16110131.

Emeis S. 2005. How Well Does a Power Law Fit to a Diabatic Boundary-Layer Wind

Profile? .

Emeis S. 2013. Wind energy meteorology : atmopsheric physics for wind power generation. .

Fettweis X, Box JE, Agosta C, Amory C, Kittel C, Lang C, van As D, Machguth H, Gallée H. 2017. Reconstructions of the 1900–2015 Greenland ice sheet surface mass balance using the regional climate MAR model. *The Cryosphere*, 11(2): 1015–1033. https://doi.org/10.5194/tc-11-1015-2017.

Giorgetta MA, Jungclaus J, Reick CH, Legutke S, Bader J, Böttinger M, Brovkin V, Crueger T, Esch M, Fieg K, Glushak K, Gayler V, Haak H, Hollweg H-D, Ilyina T, Kinne S, Kornblueh L, Matei D, Mauritsen T, Mikolajewicz U, Mueller W, Notz D, Pithan F, Raddatz T, Rast S, Redler R, Roeckner E, Schmidt H, Schnur R, Segschneider J, Six KD, Stockhause M, Timmreck C, Wegner J, Widmann H, Wieners K-H, Claussen M, Marotzke J, Stevens B. 2013. Climate and carbon cycle changes from 1850 to 2100 in MPI-ESM simulations for the Coupled Model Intercomparison Project phase 5. *Journal of Advances in Modeling Earth Systems*, 5(3): 572–597. https://doi.org/10.1002/jame.20038.

Gruber K, Regner P, Wehrle S, Zeyringer M, Schmidt J. 2022. Towards global validation of wind power simulations: A multi-country assessment of wind power simulation from MERRA-2 and ERA-5 reanalyses bias-corrected with the global wind atlas. *Energy*, 238: 121520. https://doi.org/https://doi.org/10.1016/j.energy.2021.121520.

Gutjahr O, Heinemann G. 2018. A model-based comparison of extreme winds in the Arctic and around Greenland. *International Journal of Climatology*, 38(14): 5272–5292. https://doi.org/https://doi.org/10.1002/joc.5729.

Haas R, Pinto JG, Born K. 2014a. Can dynamically downscaled windstorm footprints be improved by observations through a probabilistic approach? *Journal of Geophysical Research*, 119(2): 713–725. https://doi.org/10.1002/2013JD020882.

Haas R, Pinto JG, Born K. 2014b. Can dynamically downscaled windstorm footprints be improved by observations through a probabilistic approach? *Journal of Geophysical Research: Atmospheres*. John Wiley & Sons, Ltd, 119(2): 713–725. https://doi.org/https://doi.org/10.1002/2013JD020882.

Hazeleger W, Severijns C, Semmler T, Ştefănescu S, Yang S, Wang X, Wyser K, Dutra

E, Baldasano JM, Bintanja R, Bougeault P, Caballero R, Ekman AML, Christensen JH, Van Den Hurk B, Jimenez P, Jones C, Kållberg P, Koenigk T, McGrath R, Miranda P, Van Noije T, Palmer T, Parodi JA, Schmith T, Selten F, Storelvmo T, Sterl A, Tapamo H, Vancoppenolle M, Viterbo P, Willén U. 2012. EC-Earth: A seamless Earth-system prediction approach in action. *Climate Dynamics*, 39(11): 2609–2610. https://doi.org/10.1175/2010BAMS2877.1.

Heinemann G, Drüe C, Makshtas A. 2022. A Three-Year Climatology of the Wind Field Structure at Cape Baranova (Severnaya Zemlya, Siberia) from SODAR Observations and High-Resolution Regional Climate Model Simulations during YOPP. *Atmosphere*, 13(6). https://doi.org/10.3390/atmos13060957.

Hersbach H, Bell B, Berrisford P, Hirahara S, Horányi A, Muñoz-Sabater J, Nicolas J, Peubey C, Radu R, Schepers D, Simmons A, Soci C, Abdalla S, Abellan X, Balsamo G, Bechtold P, Biavati G, Bidlot J, Bonavita M, De Chiara G, Dahlgren P, Dee D, Diamantakis M, Dragani R, Flemming J, Forbes R, Fuentes M, Geer A, Haimberger L, Healy S, Hogan RJ, Hólm E, Janisková M, Keeley S, Laloyaux P, Lopez P, Lupu C, Radnoti G, de Rosnay P, Rozum I, Vamborg F, Villaume S, Thépaut J-N. 2020. The ERA5 global reanalysis. *Quarterly Journal of the Royal Meteorological Society*. John Wiley & Sons, Ltd, 146(730): 1999–2049. https://doi.org/https://doi.org/10.1002/qj.3803.

Hosking JS, MacLeod D, Phillips T, Holmes CR, Watson P, Shuckburgh EF, Mitchell D. 2018. Changes in European wind energy generation potential within a 1.5{\hspace{0.167em}}{\textdegree}C warmer world. *Environmental Research Letters*. {IOP} Publishing, 13(5): 54032. https://doi.org/10.1088/1748-9326/aabf78.

Hueging H, Haas R, Born K, Jacob D, Pinto JG. 2013. Regional changes in wind energy potential over Europe using regional climate model ensemble projections. *Journal of Applied Meteorology and Climatology*, 52(4): 903–917. https://doi.org/10.1175/JAMC-D-12-086.1.

IPCC, 2021: Climate Change 2021: The Physical Science Basis. Contribution of Working Group I to the Sixth Assessment Report of the Intergovernmental Panel on Climate Change [Masson-Delmotte, V., P. Zhai, A. Pirani, S.L. Connors, C. Péan, S. Berger, N. Caud, Y. Chen, L. Goldfarb, M.I. Gomis, M. Huang, K. Leitzell, E. Lonnoy, J.B.R. Matthews, T.K. Maycock, T. Waterfield, O. Yelekçi, R. Yu, and B. Zhou (eds.)].

Cambridge University Press, Cambridge, United Kingdom and New York, NY, USA, 2391 pp. doi:10.1017/9781009157896.

Jakobson L, Vihma T, Jakobson E. 2019. Relationships between sea ice concentration and wind speed over the Arctic Ocean during 1979–2015. *Journal of Climate*, 32(22): 7783–7796. https://doi.org/10.1175/JCLI-D-19-0271.1.

Jansen E, Christensen JH, Dokken T, Nisancioglu KH, Vinther BM, Capron E, Guo C, Jensen MF, Langen PL, Pedersen RA, Yang S, Bentsen M, Kjær HA, Sadatzki H, Sessford E, Stendel M. 2020. Past perspectives on the present era of abrupt Arctic climate change. *Nature Climate Change*, 10(8): 714–721. https://doi.org/10.1038/s41558-020-0860-7.

Jung C, Schindler D. 2022. A review of recent studies on wind resource projections under climate change. *Renewable and Sustainable Energy Reviews*, 165: 112596. https://doi.org/https://doi.org/10.1016/j.rser.2022.112596.

Khon VC, Mokhov II, Semenov VA. 2017. Transit navigation through Northern Sea Route from satellite data and CMIP5 simulations. *Environmental Research Letters*. IOP Publishing, 12(2): 24010. https://doi.org/10.1088/1748-9326/aa5841.

Kibanova O V, Eliseev A V, Mokhov II, Khon VC. 2018. Variations in the Duration of the Navigation Period along the Northern Sea Route in the 21st Century Based on Simulations with an Ensemble of Climatic Models: Bayesian Estimates. *Doklady Earth Sciences*, 481(1): 907–911. https://doi.org/10.1134/S1028334X18070073.

Klaus D, Dethloff K, Dorn W, Rinke A, Wu DL. 2016. New insight of Arctic cloud parameterization from regional climate model simulations, satellite-based, and drifting station data. *Geophysical Research Letters*, 43(10): 5450–5459. https://doi.org/10.1002/2015GL067530.

Koenigk T, Berg P, Döscher R. 2015. Arctic climate change in an ensemble of regional CORDEX simulations. *Polar Research*, 34(2015): 1–19. https://doi.org/10.3402/polar.v34.24603.

Koenigk T, Brodeau L, Graversen RG, Karlsson J, Svensson G, Tjernström M, Willén U, Wyser K. 2013. Arctic climate change in 21st century CMIP5 simulations with EC-Earth. *Climate Dynamics*, 40(11): 2719–2743. https://doi.org/10.1007/s00382-012-1505-y.

Lambin C, Fettweis X, Kittel C, Fonder M, Ernst D. (n.d.). Assessment of future wind speed and wind power changes over South Greenland using the Modèle Atmosphérique Régional regional climate model. *International Journal of Climatology*, n/a(n/a). https://doi.org/https://doi.org/10.1002/joc.7795.

Laurila TK, Sinclair VA, Gregow H. 2021. Climatology, variability, and trends in near-surface wind speeds over the North Atlantic and Europe during 1979–2018 based on ERA5. *International Journal of Climatology*. John Wiley & Sons, Ltd, 41(4): 2253–2278. https://doi.org/10.1002/joc.6957.

Li D, Feng J, Dosio A, Qi J, Xu Z, Yin B. 2020. Historical Evaluation and Future Projections of 100-m Wind Energy Potentials Over CORDEX-East Asia. *Journal of Geophysical Research: Atmospheres*, 125(15): 1–18. https://doi.org/10.1029/2020JD032874.

Li D, Feng J, Xu Z, Yin B, Shi H, Qi J. 2019a. Statistical Bias Correction for Simulated Wind Speeds Over CORDEX-East Asia. *Earth and Space Science*, 6(2): 200–211. https://doi.org/10.1029/2018EA000493.

Li D, Feng J, Xu Z, Yin B, Shi H, Qi J. 2019b. Statistical Bias Correction for Simulated Wind Speeds Over CORDEX-East Asia. *Earth and Space Science*. John Wiley & Sons, Ltd, 6(2): 200–211. https://doi.org/https://doi.org/10.1029/2018EA000493.

Lucas-Picher P, Wulff-Nielsen M, Christensen JH, Aðalgeirsdóttir G, Mottram R, Simonsen SB. 2012. Very high resolution regional climate model simulations over Greenland: Identifying added value. *Journal of Geophysical Research: Atmospheres*, 117(D2): n/a-n/a. https://doi.org/10.1029/2011JD016267.

Lüpkes C, Gryanik VM, Rösel A, Birnbaum G, Kaleschke L. 2013. Effect of sea ice morphology during Arctic summer on atmospheric drag coefficients used in climate models. *Geophysical Research Letters*, 40(2): 446–451. https://doi.org/https://doi.org/10.1002/grl.50081.

Martynov A, Laprise R, Sushama L, Winger K, Šeparović L, Dugas B. 2013. Reanalysis-driven climate simulation over CORDEX North America domain using the Canadian Regional Climate Model, version 5: model performance evaluation. *Climate Dynamics*, 41(11–12): 2973–3005. https://doi.org/10.1007/s00382-013-1778-9.

Massonnet F, Fichefet T, Goosse H, Bitz CM, Philippon-Berthier G, Holland MM, Barriat P-Y. 2012. Constraining projections of summer Arctic sea ice. *The Cryosphere*, 6(6): 1383–1394. https://doi.org/10.5194/tc-6-1383-2012.

McKenna R, Ostman P, Fichtner W. 2016. Key challenges and prospects for large wind turbines. *Renewable and Sustainable Energy Reviews*. Elsevier Ltd, 1212–1221.

Minola L, Zhang F, Azorin-Molina C, Pirooz AAS, Flay RGJ, Hersbach H, Chen D. 2020. Near-surface mean and gust wind speeds in ERA5 across Sweden: towards an improved gust parametrization. *Climate Dynamics*, 55(3): 887–907. https://doi.org/10.1007/s00382-020-05302-6.

Mioduszewski J, Vavrus S, Wang M. 2018. Diminishing Arctic Sea Ice Promotes Stronger Surface Winds. *Journal of Climate*. American Meteorological Society: Boston MA, USA, 31(19): 8101–8119. https://doi.org/10.1175/JCLI-D-18-0109.1.

Moemken J, Reyers M, Feldmann H, Pinto JG. 2018. Future Changes of Wind Speed and Wind Energy Potentials in EURO-CORDEX Ensemble Simulations. *Journal of Geophysical Research: Atmospheres*, 123(12): 6373–6389. https://doi.org/10.1029/2018JD028473.

Olauson J. 2018. ERA5: The new champion of wind power modelling? *Renewable Energy*, 126: 322–331. https://doi.org/https://doi.org/10.1016/j.renene.2018.03.056.

Pearson RG, Phillips SJ, Loranty MM, Beck PSA, Damoulas T, Knight SJ, Goetz SJ. 2013. Shifts in Arctic vegetation and associated feedbacks under climate change. *Nature Climate Change*, 3(7): 673–677. https://doi.org/10.1038/nclimate1858.

Pryor SC, Schoof JT, Barthelmie RJ. 2005. Empirical downscaling of wind speed probability distributions. *Journal of Geophysical Research: Atmospheres*. John Wiley & Sons, Ltd, 110(D19). https://doi.org/https://doi.org/10.1029/2005JD005899.

Ramon J, Lledó L, Torralba V, Soret A, Doblas-Reyes FJ. 2019. What global reanalysis best represents near-surface winds? *Quarterly Journal of the Royal Meteorological Society*. John Wiley & Sons, Ltd, 145(724): 3236–3251. https://doi.org/https://doi.org/10.1002/qj.3616.

Rantanen M, Karpechko AY, Lipponen A, Nordling K, Hyvärinen O, Ruosteenoja K, Vihma T, Laaksonen A. 2022. The Arctic has warmed nearly four times faster than the globe since 1979. *Communications Earth & Environment*, 3(1): 168. https://doi.org/10.1038/s43247-022-00498-3.

Semenov VA, Latif M. 2015. Nonlinear winter atmospheric circulation response to Arctic sea ice concentration anomalies for different periods during 1966 – 2012 Nonlinear winter atmospheric circulation response to Arctic sea ice concentration anomalies for different periods during 1. IOP Publishing. https://doi.org/10.1088/1748-9326/10/5/054020.

Šeparović L, Alexandru A, Laprise R, Martynov A, Sushama L, Winger K, Tete K, Valin M. 2013. Present climate and climate change over North America as simulated by the fifth-generation Canadian regional climate model. *Climate Dynamics*, 41(11–12): 3167–3201. https://doi.org/10.1007/s00382-013-1737-5.

Smith B, Samuelsson P, Wramneby A, Rummukainen M. 2011. A model of the coupled dynamics of climate, vegetation and terrestrial ecosystem biogeochemistry for regional applications. *Tellus, Series A: Dynamic Meteorology and Oceanography*, 63(1): 87–106. https://doi.org/10.1111/j.1600-0870.2010.00477.x.

Soares PMM, Lima DCA, Nogueira M. 2020. Global offshore wind energy resources using the new {ERA}-5 reanalysis. *Environmental Research Letters*. {IOP} Publishing, 15(10): 1040a2. https://doi.org/10.1088/1748-9326/abb10d.

Sommerfeld A, Nikiema O, Rinke A, Dethloff K, Laprise R. 2015. Arctic budget study of intermember variability using HIRHAM5 ensemble simulations. *Journal of Geophysical Research: Atmospheres*, 120(18): 9390–9407. https://doi.org/10.1002/2015JD023153.

Takhsha M, Nikiéma O, Lucas-Picher P, Laprise R, Hernández-Díaz L, Winger K. 2017. Dynamical downscaling with the fifth-generation Canadian regional climate model (CRCM5) over the CORDEX Arctic domain: effect of large-scale spectral nudging and of empirical correction of sea-surface temperature. *Climate Dynamics*. Springer Berlin Heidelberg, 0(0): 1–26. https://doi.org/10.1007/s00382-017-3912-6.

Taylor KE, Stouffer RJ, Meehl GA. 2012. An overview of CMIP5 and the experiment design. *Bulletin of the American Meteorological Society*, 93(4): 485–498. https://doi.org/10.1175/BAMS-D-11-00094.1.

Tobin I, Vautard R, Balog I, Bréon F-M, Jerez S, Ruti P, Thais F, Vrac M, Yiou P. 2015. Assessing climate change impacts on European wind energy from ENSEMBLES high-resolution climate projections. *Climatic Change*, 128(1): 99–112. https://doi.org/10.1007/s10584-014-1291-0.

Tuononen M, Sinclair VA, Vihma T. 2015. A climatology of low-level jets in the mid-latitudes and polar regions of the Northern Hemisphere. *Atmospheric Science Letters*, 16(4): 492–499. https://doi.org/https://doi.org/10.1002/asl.587.

Vavrus SJ, Alkama R. 2021. Future trends of arctic surface wind speeds and their relationship with sea ice in CMIP5 climate model simulations. *Climate Dynamics*. Springer Berlin Heidelberg, (0123456789). https://doi.org/10.1007/s00382-021-06071-6.

Vihma T. 2014. *Effects of Arctic Sea Ice Decline on Weather and Climate: A Review*. *Surveys in Geophysics*.

Zhang W, Jansson C, Miller PA, Smith B, Samuelsson P. 2014. Biogeophysical feedbacks enhance the Arctic terrestrial carbon sink in regional Earth system dynamics. *Biogeosciences*, 11(19): 5503–5519. https://doi.org/10.5194/bg-11-5503-2014.

Zhang W, Miller PA, Jansson C, Samuelsson P, Mao J, Smith B. 2018. Self-Amplifying Feedbacks Accelerate Greening and Warming of the Arctic. *Geophysical Research Letters*, 45(14): 7102–7111. https://doi.org/10.1029/2018GL077830.